

Measurements of multiparticle correlations in d +Au collisions at 200, 62.4, 39, and 19.6 GeV and p +Au collisions at 200 GeV and implications for collective behavior

C. Aidala,⁴⁰ Y. Akiba,^{51,52,*} M. Alfred,²² V. Andrieux,⁴⁰ K. Aoki,³⁰ N. Apadula,²⁷ H. Asano,^{33,51} C. Ayuso,⁴⁰ B. Azmoun,⁷ V. Babintsev,²³ A. Bagoly,¹⁶ N.S. Bandara,³⁹ K.N. Barish,⁸ S. Bathe,^{5,52} A. Bazilevsky,⁷ M. Beaumier,⁸ R. Belmont,¹² A. Berdnikov,⁵⁴ Y. Berdnikov,⁵⁴ D.S. Blau,³² M. Boer,³⁵ J.S. Bok,⁴⁵ M.L. Brooks,³⁵ J. Bryslawskij,^{5,8} V. Bumazhnov,²³ C. Butler,²⁰ S. Campbell,¹³ V. Canoa Roman,⁵⁷ R. Cervantes,⁵⁷ C.Y. Chi,¹³ M. Chiu,⁷ I.J. Choi,²⁴ J.B. Choi,^{10,†} Z. Citron,⁶² M. Connors,^{20,52} N. Cronin,⁵⁷ M. Csanád,¹⁶ T. Csörgő,^{17,63} T.W. Danley,⁴⁶ M.S. Daugherty,¹ G. David,^{7,57} K. DeBlasio,⁴⁴ K. Dehmelt,⁵⁷ A. Denisov,²³ A. Deshpande,^{52,57} E.J. Desmond,⁷ A. Dion,⁵⁷ D. Dixit,⁵⁷ J.H. Do,⁶⁴ A. Drees,⁵⁷ K.A. Drees,⁶ M. Dumancic,⁶² J.M. Durham,³⁵ A. Durum,²³ T. Elder,²⁰ A. Enokizono,^{51,53} H. En'yo,⁵¹ S. Esumi,⁶⁰ B. Fadem,⁴¹ W. Fan,⁵⁷ N. Feege,⁵⁷ D.E. Fields,⁴⁴ M. Finger,⁹ M. Finger, Jr.,⁹ S.L. Fokin,³² J.E. Frantz,⁴⁶ A. Franz,⁷ A.D. Frawley,¹⁹ Y. Fukuda,⁶⁰ C. Gal,⁵⁷ P. Gallus,¹⁴ P. Garg,^{3,57} H. Ge,⁵⁷ F. Giordano,²⁴ Y. Goto,^{51,52} N. Grau,² S.V. Greene,⁶¹ M. Grosse Perdekamp,²⁴ T. Gunji,¹¹ H. Guragain,²⁰ T. Hachiya,^{51,52} J.S. Haggerty,⁷ K.I. Hahn,¹⁸ H. Hamagaki,¹¹ H.F. Hamilton,¹ S.Y. Han,¹⁸ J. Hanks,⁵⁷ S. Hasegawa,²⁸ T.O.S. Haseler,²⁰ X. He,²⁰ T.K. Hemmick,⁵⁷ J.C. Hill,²⁷ K. Hill,¹² A. Hodges,²⁰ R.S. Hollis,⁸ K. Homma,²¹ B. Hong,³¹ T. Hoshino,²¹ N. Hotvedt,²⁷ J. Huang,⁷ S. Huang,⁶¹ K. Imai,²⁸ J. Imrek,¹⁵ M. Inaba,⁶⁰ A. Iordanova,⁸ D. Isenhower,¹ Y. Ito,⁴² D. Ivanishchev,⁵⁰ B.V. Jacak,⁵⁷ M. Jezghani,²⁰ Z. Ji,⁵⁷ X. Jiang,³⁵ B.M. Johnson,^{7,20} V. Jorjadze,⁵⁷ D. Jouan,⁴⁸ D.S. Jumper,²⁴ J.H. Kang,⁶⁴ D. Kapukchyan,⁸ S. Karthas,⁵⁷ D. Kawall,³⁹ A.V. Kazantsev,³² V. Khachatryan,⁵⁷ A. Khanzadeev,⁵⁰ C. Kim,^{8,31} D.J. Kim,²⁹ E.-J. Kim,¹⁰ M. Kim,⁵⁵ M.H. Kim,³¹ D. Kincses,¹⁶ E. Kistenev,⁷ J. Klatsky,¹⁹ P. Kline,⁵⁷ T. Koblesky,¹² D. Kotov,^{50,54} S. Kudo,⁶⁰ K. Kurita,⁵³ Y. Kwon,⁶⁴ J.G. Lajoie,²⁷ E.O. Lallow,⁴¹ A. Lebedev,²⁷ S. Lee,⁶⁴ S.H. Lee,^{27,57} M.J. Leitch,³⁵ Y.H. Leung,⁵⁷ N.A. Lewis,⁴⁰ X. Li,³⁵ S.H. Lim,^{35,64} L. D. Liu,⁴⁹ M.X. Liu,³⁵ V.-R. Loggins,²⁴ S. Lökös,^{16,17} K. Lovasz,¹⁵ D. Lynch,⁷ T. Majoros,¹⁵ Y.I. Makdisi,⁶ M. Makek,⁶⁵ M. Malaev,⁵⁰ V.I. Manko,³² E. Mannel,⁷ H. Masuda,⁵³ M. McCumber,³⁵ P.L. McGaughey,³⁵ D. McGlinchey,^{12,35} C. McKinney,²⁴ M. Mendoza,⁸ W.J. Metzger,¹⁷ A.C. Mignerey,³⁸ D.E. Mihalik,⁵⁷ A. Milov,⁶² D.K. Mishra,⁴ J.T. Mitchell,⁷ G. Mitsuka,⁵² S. Miyasaka,^{51,59} S. Mizuno,^{51,60} P. Montuenga,²⁴ T. Moon,⁶⁴ D.P. Morrison,⁷ S.I.M. Morrow,⁶¹ T. Murakami,^{33,51} J. Murata,^{51,53} K. Nagai,⁵⁹ K. Nagashima,²¹ T. Nagashima,⁵³ J.L. Nagle,¹² M.I. Nagy,¹⁶ I. Nakagawa,^{51,52} H. Nakagomi,^{51,60} K. Nakano,^{51,59} C. Nattrass,⁵⁸ T. Niida,⁶⁰ R. Nouicer,^{7,52} T. Novák,^{17,63} N. Novitzky,⁵⁷ R. Novotny,¹⁴ A.S. Nyanin,³² E. O'Brien,⁷ C.A. Ogilvie,²⁷ J.D. Orjuela Koop,¹² J.D. Osborn,⁴⁰ A. Oskarsson,³⁶ G.J. Ottino,⁴⁴ K. Ozawa,^{30,60} V. Pantuev,²⁵ V. Papavassiliou,⁴⁵ J.S. Park,⁵⁵ S. Park,^{51,55,57} S.F. Pate,⁴⁵ M. Patel,²⁷ W. Peng,⁶¹ D.V. Perpelitsa,^{7,12} G.D.N. Perera,⁴⁵ D.Yu. Peressounko,³² C.E. PerezLara,⁵⁷ J. Perry,²⁷ R. Petti,⁷ M. Phipps,^{7,24} C. Pinkenburg,⁷ R.P. Pisani,⁷ A. Pun,⁴⁶ M.L. Purschke,⁷ P.V. Radzevich,⁵⁴ K.F. Read,^{47,58} D. Reynolds,⁵⁶ V. Riabov,^{43,50} Y. Riabov,^{50,54} D. Richford,⁵ T. Rinn,²⁷ S.D. Rolnick,⁸ M. Rosati,²⁷ Z. Rowan,⁵ J. Runchey,²⁷ A.S. Safonov,⁵⁴ T. Sakaguchi,⁷ H. Sako,²⁸ V. Samsonov,^{43,50} M. Sarsour,²⁰ K. Sato,⁶⁰ S. Sato,²⁸ B. Schaefer,⁶¹ B.K. Schmoll,⁵⁸ K. Sedgwick,⁸ R. Seidl,^{51,52} A. Sen,^{27,58} R. Seto,⁸ A. Sexton,³⁸ D. Sharma,⁵⁷ I. Shein,²³ T.-A. Shibata,^{51,59} K. Shigaki,²¹ M. Shimomura,^{27,42} T. Shioya,⁶⁰ P. Shukla,⁴ A. Sickles,²⁴ C.L. Silva,³⁵ D. Silvermyr,³⁶ B.K. Singh,³ C.P. Singh,³ V. Singh,³ M.J. Skoby,⁴⁰ M. Slunečka,⁹ K.L. Smith,¹⁹ M. Snowball,³⁵ R.A. Soltz,³⁴ W.E. Sondheim,³⁵ S.P. Sorensen,⁵⁸ I.V. Sourikova,⁷ P.W. Stankus,⁴⁷ S.P. Stoll,⁷ T. Sugitate,²¹ A. Sukhanov,⁷ T. Sumita,⁵¹ J. Sun,⁵⁷ S. Syed,²⁰ J. Sziklai,⁶³ A. Takeda,⁴² K. Tanida,^{28,52,55} M.J. Tannenbaum,⁷ S. Tarafdar,^{61,62} G. Tarnai,¹⁵ R. Tieulent,^{20,37} A. Timilsina,²⁷ T. Todoroki,⁶⁰ M. Tomášek,¹⁴ C.L. Towell,¹ R.S. Towell,¹ I. Tserruya,⁶² Y. Ueda,²¹ B. Ujvari,¹⁵ H.W. van Hecke,³⁵ S. Vazquez-Carson,¹² J. Velkovska,⁶¹ M. Virius,¹⁴ V. Vrba,^{14,26} N. Vukman,⁶⁵ X.R. Wang,^{45,52} Z. Wang,⁵ Y. Watanabe,^{51,52} Y.S. Watanabe,¹¹ C.P. Wong,²⁰ C.L. Woody,⁷ C. Xu,⁴⁵ Q. Xu,⁶¹ L. Xue,²⁰ S. Yalcin,⁵⁷ Y.L. Yamaguchi,^{52,57} H. Yamamoto,⁶⁰ A. Yanovich,²³ P. Yin,¹² J.H. Yoo,³¹ I. Yoon,⁵⁵ H. Yu,^{45,49} I.E. Yushmanov,³² W.A. Zajc,¹³ A. Zelenski,⁶ S. Zharko,⁵⁴ and L. Zou⁸

(PHENIX Collaboration)

¹Abilene Christian University, Abilene, Texas 79699, USA

²Department of Physics, Augustana University, Sioux Falls, South Dakota 57197, USA

³Department of Physics, Banaras Hindu University, Varanasi 221005, India

⁴Bhabha Atomic Research Centre, Bombay 400 085, India

⁵Baruch College, City University of New York, New York, New York, 10010 USA

⁶Collider-Accelerator Department, Brookhaven National Laboratory, Upton, New York 11973-5000, USA

- ⁷ *Physics Department, Brookhaven National Laboratory, Upton, New York 11973-5000, USA*
- ⁸ *University of California-Riverside, Riverside, California 92521, USA*
- ⁹ *Charles University, Ovocný trh 5, Praha 1, 116 36, Prague, Czech Republic*
- ¹⁰ *Chonbuk National University, Jeonju, 561-756, Korea*
- ¹¹ *Center for Nuclear Study, Graduate School of Science, University of Tokyo, 6-3-1 Hongo, Bunkyo, Tokyo 113-0033, Japan*
- ¹² *University of Colorado, Boulder, Colorado 80309, USA*
- ¹³ *Columbia University, New York, New York 10027 and Nevis Laboratories, Irvington, New York 10533, USA*
- ¹⁴ *Czech Technical University, Zikova 4, 166 36 Prague 6, Czech Republic*
- ¹⁵ *Debrecen University, H-4010 Debrecen, Egyetem tér 1, Hungary*
- ¹⁶ *ELTE, Eötvös Loránd University, H-1117 Budapest, Pázmány P. s. 1/A, Hungary*
- ¹⁷ *Eszterházy Károly University, Károly Róbert Campus, H-3200 Gyöngyös, Mátrai út 36, Hungary*
- ¹⁸ *Ewha Womans University, Seoul 120-750, Korea*
- ¹⁹ *Florida State University, Tallahassee, Florida 32306, USA*
- ²⁰ *Georgia State University, Atlanta, Georgia 30303, USA*
- ²¹ *Hiroshima University, Kagamiyama, Higashi-Hiroshima 739-8526, Japan*
- ²² *Department of Physics and Astronomy, Howard University, Washington, DC 20059, USA*
- ²³ *IHEP Protvino, State Research Center of Russian Federation, Institute for High Energy Physics, Protvino, 142281, Russia*
- ²⁴ *University of Illinois at Urbana-Champaign, Urbana, Illinois 61801, USA*
- ²⁵ *Institute for Nuclear Research of the Russian Academy of Sciences, prospekt 60-letiya Oktyabrya 7a, Moscow 117312, Russia*
- ²⁶ *Institute of Physics, Academy of Sciences of the Czech Republic, Na Slovance 2, 182 21 Prague 8, Czech Republic*
- ²⁷ *Iowa State University, Ames, Iowa 50011, USA*
- ²⁸ *Advanced Science Research Center, Japan Atomic Energy Agency, 2-4 Shirakata Shirane, Tokai-mura, Naka-gun, Ibaraki-ken 319-1195, Japan*
- ²⁹ *Helsinki Institute of Physics and University of Jyväskylä, P.O.Box 35, FI-40014 Jyväskylä, Finland*
- ³⁰ *KEK, High Energy Accelerator Research Organization, Tsukuba, Ibaraki 305-0801, Japan*
- ³¹ *Korea University, Seoul, 136-701, Korea*
- ³² *National Research Center “Kurchatov Institute”, Moscow, 123098 Russia*
- ³³ *Kyoto University, Kyoto 606-8502, Japan*
- ³⁴ *Lawrence Livermore National Laboratory, Livermore, California 94550, USA*
- ³⁵ *Los Alamos National Laboratory, Los Alamos, New Mexico 87545, USA*
- ³⁶ *Department of Physics, Lund University, Box 118, SE-221 00 Lund, Sweden*
- ³⁷ *IPNL, CNRS/IN2P3, Univ Lyon, Universit Lyon 1, F-69622, Villeurbanne, France*
- ³⁸ *University of Maryland, College Park, Maryland 20742, USA*
- ³⁹ *Department of Physics, University of Massachusetts, Amherst, Massachusetts 01003-9337, USA*
- ⁴⁰ *Department of Physics, University of Michigan, Ann Arbor, Michigan 48109-1040, USA*
- ⁴¹ *Muhlenberg College, Allentown, Pennsylvania 18104-5586, USA*
- ⁴² *Nara Women’s University, Kita-uoya Nishi-machi Nara 630-8506, Japan*
- ⁴³ *National Research Nuclear University, MEPhI, Moscow Engineering Physics Institute, Moscow, 115409, Russia*
- ⁴⁴ *University of New Mexico, Albuquerque, New Mexico 87131, USA*
- ⁴⁵ *New Mexico State University, Las Cruces, New Mexico 88003, USA*
- ⁴⁶ *Department of Physics and Astronomy, Ohio University, Athens, Ohio 45701, USA*
- ⁴⁷ *Oak Ridge National Laboratory, Oak Ridge, Tennessee 37831, USA*
- ⁴⁸ *IPN-Orsay, Univ. Paris-Sud, CNRS/IN2P3, Université Paris-Saclay, BP1, F-91406, Orsay, France*
- ⁴⁹ *Peking University, Beijing 100871, People’s Republic of China*
- ⁵⁰ *PNPI, Petersburg Nuclear Physics Institute, Gatchina, Leningrad region, 188300, Russia*
- ⁵¹ *RIKEN Nishina Center for Accelerator-Based Science, Wako, Saitama 351-0198, Japan*
- ⁵² *RIKEN BNL Research Center, Brookhaven National Laboratory, Upton, New York 11973-5000, USA*
- ⁵³ *Physics Department, Rikkyo University, 3-34-1 Nishi-Ikebukuro, Toshima, Tokyo 171-8501, Japan*
- ⁵⁴ *Saint Petersburg State Polytechnic University, St. Petersburg, 195251 Russia*
- ⁵⁵ *Department of Physics and Astronomy, Seoul National University, Seoul 151-742, Korea*
- ⁵⁶ *Chemistry Department, Stony Brook University, SUNY, Stony Brook, New York 11794-3400, USA*
- ⁵⁷ *Department of Physics and Astronomy, Stony Brook University, SUNY, Stony Brook, New York 11794-3800, USA*
- ⁵⁸ *University of Tennessee, Knoxville, Tennessee 37996, USA*
- ⁵⁹ *Department of Physics, Tokyo Institute of Technology, Oh-okayama, Meguro, Tokyo 152-8551, Japan*
- ⁶⁰ *Center for Integrated Research in Fundamental Science and Engineering, University of Tsukuba, Tsukuba, Ibaraki 305, Japan*
- ⁶¹ *Vanderbilt University, Nashville, Tennessee 37235, USA*
- ⁶² *Weizmann Institute, Rehovot 76100, Israel*
- ⁶³ *Institute for Particle and Nuclear Physics, Wigner Research Centre for Physics, Hungarian Academy of Sciences (Wigner RCP, RMKI) H-1525 Budapest 114, POBox 49, Budapest, Hungary*
- ⁶⁴ *Yonsei University, IPAP, Seoul 120-749, Korea*
- ⁶⁵ *Department of Physics, Faculty of Science, University of Zagreb, Bijenička c. 32 HR-10002 Zagreb, Croatia*

(Dated: August 11, 2019)

Recently, multiparticle-correlation measurements of relativistic $p/d/{}^3\text{He}+\text{Au}$, $p+\text{Pb}$, and even $p+p$ collisions have shown surprising collective signatures. Here we present beam-energy-scan measurements of 2-, 4-, and 6-particle angular correlations in $d+\text{Au}$ collisions at $\sqrt{s_{NN}} = 200, 62.4, 39,$ and 19.6 GeV. We also present measurements of 2- and 4-particle angular correlations in $p+\text{Au}$ collisions at $\sqrt{s_{NN}} = 200$ GeV. We find the 4-particle cumulant to be real-valued for $d+\text{Au}$ collisions at all four energies. We also find that the 4-particle cumulant in $p+\text{Au}$ has the opposite sign as that in $d+\text{Au}$. Further we find that the 6-particle cumulant agrees with the 4-particle cumulant in $d+\text{Au}$ collisions at 200 GeV, indicating that nonflow effects are subdominant. These observations provide strong evidence that the correlations originate from the initial geometric configuration which is then translated into the momentum distribution for all particles, commonly referred to as collectivity.

One of the key discoveries at the Relativistic Heavy Ion Collider (RHIC) is the identification of the quark-gluon plasma (QGP) and its characterization as a near perfect fluid via its collective flow [1–4]. It has previously been assumed that only nucleus-on-nucleus collisions create a system large enough and hot enough to create the QGP. However, five years ago, collective signatures were discovered in $p+\text{Pb}$ collisions at $\sqrt{s_{NN}} = 5.02$ TeV at the large hadron collider (LHC) [5–7]. Since then, similar evidence has been observed in $p/d/{}^3\text{He}+\text{Au}$ collisions at $\sqrt{s_{NN}} = 200$ GeV at RHIC [8–11] and high-multiplicity $p+p$ collisions at $\sqrt{s_{NN}} = 2.76\text{--}13$ TeV at the LHC [12–14]. Additionally, collective signatures at the LHC have been found not only with 2-particle correlations, but with multiparticle correlations as well [15–18]. Multiparticle correlations are not a unique signature of a hydrodynamically flowing medium [19, 20], and thus it is imperative that all calculational frameworks make quantitative predictions for these correlations. This Letter presents the measurement of multiparticle correlations in $d+\text{Au}$ collisions as part of a beam energy scan at $\sqrt{s_{NN}} = 200, 62.4, 39,$ and 19.6 GeV, as well as in $p+\text{Au}$ collisions at $\sqrt{s_{NN}} = 200$ GeV.

The azimuthal distribution of particles produced in a collision can be described by a Fourier series with harmonic coefficients v_n where n is the harmonic number [21]. This analysis uses direct calculations of cumulants [22]. The 2-particle correlator is

$$\langle 2 \rangle = \langle \cos(n(\phi_1 - \phi_2)) \rangle = \langle v_n^2 \rangle, \quad (1)$$

where $\phi_{1,2}$ denote the azimuthal angles of two different particles in a single event and the single brackets denote an average over particles in a single event. The 4-particle correlator is

$$\langle 4 \rangle = \langle \cos(n(\phi_1 + \phi_2 - \phi_3 - \phi_4)) \rangle = \langle v_n^4 \rangle, \quad (2)$$

where $\phi_{1,2,3,4}$ denote the azimuthal angles of four different particles in a single event. Finally, the 6-particle correlator is

$$\langle 6 \rangle = \langle \cos(n(\phi_1 + \phi_2 + \phi_3 - \phi_4 - \phi_5 - \phi_6)) \rangle = \langle v_n^6 \rangle, \quad (3)$$

where $\phi_{1,2,3,4,5,6}$ denote the azimuthal angles of six different particles in a single event. Quite generally, any

m -particle correlation will have contributions from lower-order correlations, and m -particle cumulants $c_n\{m\}$ are constructed to remove these. In the case of the 2-particle cumulant, the relation is simply

$$c_n\{2\} = \langle\langle 2 \rangle\rangle, \quad (4)$$

where the double bracket indicates first an average over particles in a single event and then an average over events. In the case of the 4- and 6-particle cumulant, the relations are

$$c_n\{4\} = \langle\langle 4 \rangle\rangle - 2\langle\langle 2 \rangle\rangle^2 \quad \text{and} \quad (5)$$

$$c_n\{6\} = \langle\langle 6 \rangle\rangle - 9\langle\langle 4 \rangle\rangle\langle\langle 2 \rangle\rangle + 12\langle\langle 2 \rangle\rangle^3, \quad (6)$$

where it can be seen by construction that the lower-order correlations are removed. The harmonic coefficients are related to the cumulants by

$$v_n\{2\} = (c_n\{2\})^{1/2}, \quad (7)$$

$$v_n\{4\} = (-c_n\{4\})^{1/4} \quad \text{and} \quad (8)$$

$$v_n\{6\} = \left(\frac{1}{4}c_n\{6\}\right)^{1/6}. \quad (9)$$

In this Letter we focus on the second harmonic, $n = 2$, which is interpreted as arising from elliptic flow. For a given event category, there can be event-by-event differences in the strength of the elliptic flow. In this case the observed v_2 is not a single value but rather a distribution. The different cumulants have different sensitivities to the fluctuations of the v_2 distribution. The $v_2\{2\}$ has a positive contribution from the variance of the distribution, whereas $v_2\{4\}$ and $v_2\{6\}$ have negative contributions from the variance. Comparisons of the different cumulants can yield insights into not only the central value of the v_2 but also the nature of its event-by-event fluctuations.

Not all angular correlations are global in nature. The term nonflow is used to describe angular correlations arising from anything not considered global or collective in nature, and typically includes resonance decays, quantum interference correlations, Coulomb interactions, jet correlations, etc. Most of these generate correlations among only a small subset of the total produced particles, thus 4-particle correlations are typically much less sensitive than 2-particle correlations to nonflow effects. For that

reason, comparison between 2-, 4-, and 6-particle correlations can also yield insights into nonflow effects. Considering the event-by-event v_2 fluctuations (in the Gaussian limit) and nonflow, one has

$$v_2\{2\} = (v_2^2 + \sigma^2 + \delta^2)^{1/2} \quad \text{and} \quad (10)$$

$$v_2\{4\} \approx v_2\{6\} \approx (v_2^2 - \sigma^2)^{1/2}, \quad (11)$$

where σ^2 is the variance of the distribution and δ^2 parameterizes the nonflow [23].

In 2016, the PHENIX experiment [24] at RHIC collected data from $d+Au$ collisions at four different energies ($\sqrt{s_{NN}} = 200, 62.4, 39,$ and 19.6 GeV). In 2015, data from $p+Au$ collisions at $\sqrt{s_{NN}} = 200$ GeV was collected. PHENIX triggered on minimum bias and high multiplicity events utilizing a beam beam counter (BBC) [25] at 200 and 62.4 GeV or a forward silicon detector (FVTX) [26] at 39 and 19.6 GeV. Using information from the BBC and FVTX, we require events to have a collision vertex within $|z| < 10$ cm of the nominal center of the PHENIX coordinate system.

The particle correlations are formed from reconstructed tracks in the FVTX, which has two arms covering $-3 < \eta < -1$ and $+1 < \eta < +3$ in pseudorapidity. The FVTX does not provide momentum information, but simulations have determined that the efficiency is momentum independent for $p_T \gtrsim 0.3$ GeV/ c . We require tracks in the FVTX to have a distance of closest approach (DCA) to the reconstructed vertex less than 2 cm and to have hits in at least 3 of the 4 layers of the FVTX. We evaluate all quantities as a function of the number of reconstructed tracks in the FVTX, $N_{\text{tracks}}^{\text{FVTX}}$. The $\langle\langle 6 \rangle\rangle$, $\langle\langle 4 \rangle\rangle$, and $\langle\langle 2 \rangle\rangle$ are evaluated in events categorized by a single integer value of $N_{\text{tracks}}^{\text{FVTX}}$. Event categories are then combined into wider bins as needed to achieve adequate statistical precision. As an illustrative example, $10 < N_{\text{tracks}}^{\text{FVTX}} < 30$ corresponds to centralities in $d+Au$ of 1.3%–52%, $4.1 \times 10^{-2}\%$ –33%, $6.5 \times 10^{-4}\%$ –21%, and $3.3 \times 10^{-6}\%$ –10% at 200, 62.4, 39, 19.6 GeV respectively, and in $p+Au$ at 200 GeV of 0.22%–29%.

Figure 1 shows (a,c) the $\langle\langle 4 \rangle\rangle$ and $2\langle\langle 2 \rangle\rangle^2$ and (b,c) cumulant $c_2\{4\}$ for (a,b) $p+Au$ collisions and (c,d) $d+Au$ collisions at $\sqrt{s_{NN}} = 200$ GeV. In both cases, only statistical uncertainties are shown. The cumulant in $p+Au$ is positive, indicating that $v_2\{4\}$ is complex. In contrast, in $p+Pb$ collisions at $\sqrt{s_{NN}} = 5.02$ TeV, the cumulant is negative and the $v_2\{4\}$ is real for sufficiently high multiplicity [15–18]. However, the cumulant in $d+Au$ collisions at $\sqrt{s_{NN}} = 200$ GeV is negative, indicating that $v_2\{4\}$ is real. For now, we focus on the $d+Au$ results and will return to the $p+Au$ system later.

Figure 2 shows the calculated $v_2\{2\}$ and $v_2\{4\}$ in $d+Au$ collisions at 200, 62.4, 39, and 19.6 GeV. Systematic uncertainties, shown as colored bands, are point-to-point correlated and are determined as the quadrature sum of

the following contributions. We vary the event vertex cut from the 10 cm default to 5 cm as a check on the z dependence of the FVTX acceptance and find a systematic uncertainty of approximately 1% (10%) for 2-particle (4-particle) correlations. The DCA cut is varied from the default 2 cm cut to 1.5 cm, and we find a systematic difference of approximately 1%. The azimuthal acceptance in the FVTX is not uniform due to detector inefficiencies, so corrections need to be applied. We use the Q-vector recentering method [27] as the default and compare to the isotropic terms in Ref. [22]. We assess an uncertainty of 10% of the value of the $v_2\{2\}$ and $v_2\{4\}$ due to this correction, which is the dominant source of systematic uncertainty.

Rather strikingly, we observe real-valued $v_2\{4\}$ in $d+Au$ at all four collision energies. This is additional evidence in support of collective behavior in small systems [8–11]. The same patterns seen in $p+Pb$ collisions at the LHC appears to persist in $d+Au$ at collision energies a factor of 250 lower.

Further, Fig. 2 shows the $v_2\{6\}$ in $d+Au$ collisions at 200 GeV. The $v_2\{6\}$ is consistent with $v_2\{4\}$ across the full $N_{\text{tracks}}^{\text{FVTX}}$ range. This shows that, at least at 200 GeV, the $v_2\{4\}$ is dominated by flow, rather than nonflow. The statistics at the lower energies are not enough to determine a reliable $v_2\{6\}$.

Figure 3 shows the $v_2\{2\}$ and $v_2\{4\}$ in $d+Au$ collisions as a function of $\sqrt{s_{NN}}$ when averaged over $10 < N_{\text{tracks}}^{\text{FVTX}} < 30$. We find that $v_2\{4\} < v_2\{2\}$ at the higher energies, as expected from Eqns. 10, 11 where both the event-to-event v_2 fluctuations and nonflow contribute positively to $v_2\{2\}$, and the v_2 fluctuations contribute negatively to $v_2\{4\}$ while nonflow should be significantly reduced. However, there is a trend that the difference between the $v_2\{2\}$ and $v_2\{4\}$ decreases with decreasing energy, with $v_2\{2\} \approx v_2\{4\}$ within uncertainties at 19.6 and 39 GeV. If Eqns. 10, 11 are valid at these low multiplicities, the $v_2\{2\}$ and $v_2\{4\}$ may converge if the flow fluctuations (σ) or the nonflow (δ) decrease at lower $d+Au$ energies. Monte Carlo Glauber calculations indicate that the event-by-event fluctuations in the initial geometry are quite similar for $d+Au$ collisions at all four energies. In the case of nonflow, while jet contributions decrease at lower energy, the expectation is that δ increases because one has a nonflow correlation from a fixed particle number (N) that is diluted by the total number of particles in the event (M), which is smaller for lower energy $d+Au$ collisions even at fixed number of FVTX tracks. The measured 2- and 4-particle correlations appear to be more complex than the assumptions in Eqns. 10, 11.

To explore these trends in more detail, we utilize A-Multi-Phase-Transport (AMPT) model that includes parton production via string melting, parton scattering, hadronization via coalescence, and hadronic scattering [28]. AMPT has been successful at qualitatively de-

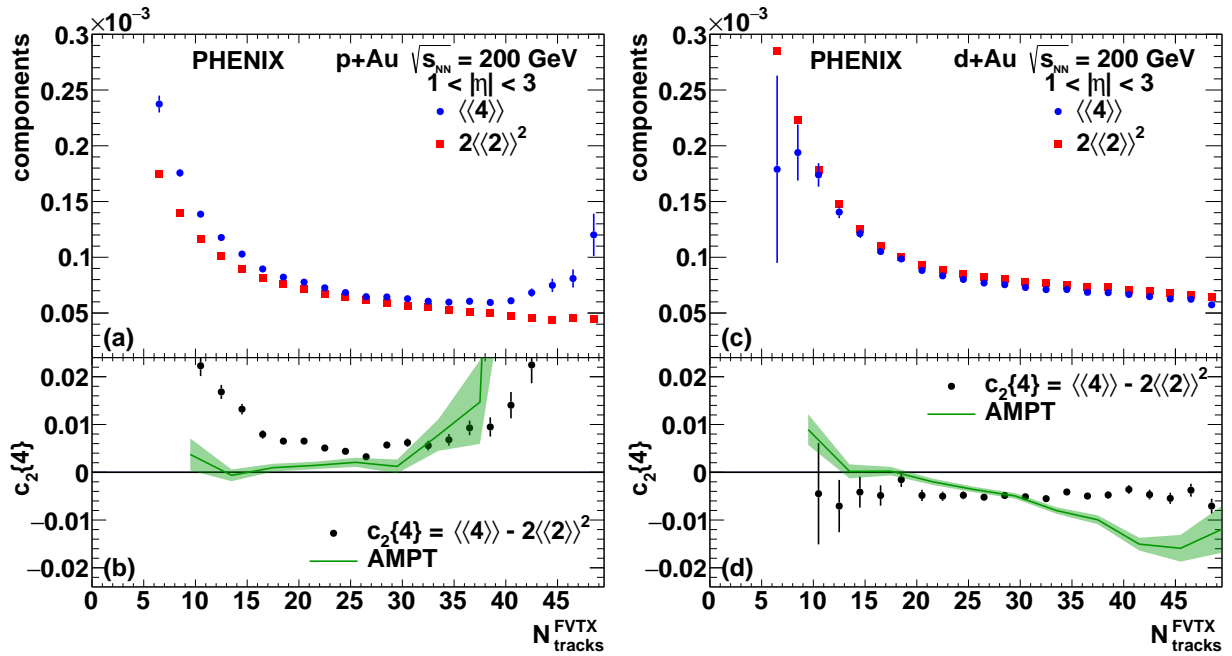


FIG. 1. Components $\langle\langle 4 \rangle\rangle$ and $2\langle\langle 2 \rangle\rangle^2$ and cumulant $c_2\{4\} = \langle\langle 4 \rangle\rangle - 2\langle\langle 2 \rangle\rangle^2$ as a function of $N_{\text{tracks}}^{\text{FVTX}}$. (a) and (b) show the components and cumulant, respectively, in p +Au collisions at $\sqrt{s_{NN}} = 200$ GeV. (c) and (d) show the components and cumulant, respectively, in d +Au collisions at $\sqrt{s_{NN}} = 200$ GeV. (b) and (d) also show the cumulant as measured in AMPT for p +Au and d +Au, respectively, indicated by the green line. The shaded green band indicates the statistical uncertainty on the AMPT values.

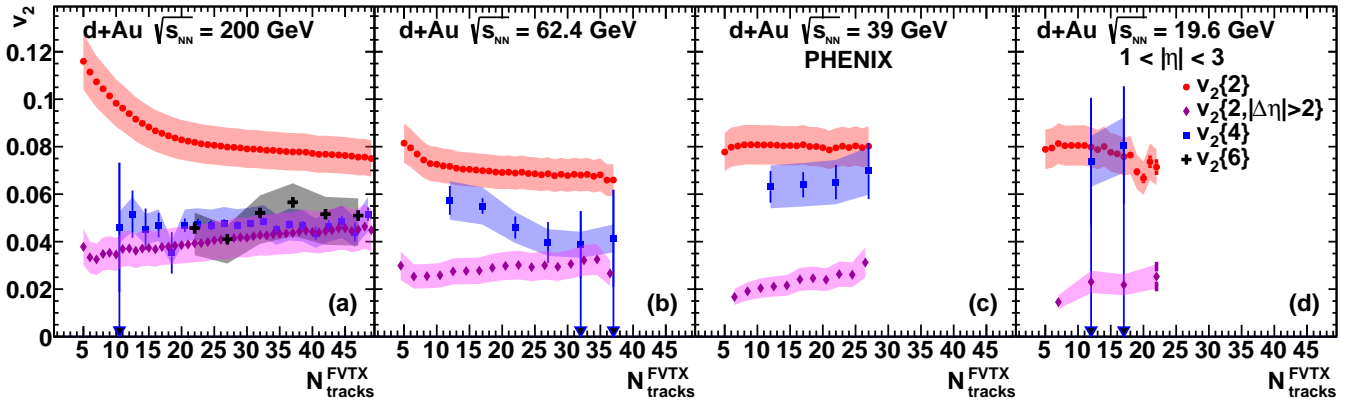


FIG. 2. $v_2\{2\}$, $v_2\{2, |\Delta\eta| > 2\}$, and $v_2\{4\}$ as a function of $N_{\text{tracks}}^{\text{FVTX}}$ in d +Au collisions with $\sqrt{s_{NN}} =$ (a) 200 GeV, (b) 62.4 GeV, (c) 39 GeV, and (d) 19.6 GeV; also shown in (a) is $v_2\{6\}$ for $\sqrt{s_{NN}} = 200$ GeV. The arrowheads on the statistical uncertainties indicate cases where the standard 1σ uncertainty on the $c_2\{4\}$ crosses zero. For 19.6 GeV, the combined confidence interval for $v_2\{4\}$ to be real is 79%.

describing many signatures of collectivity in small and large collision systems [29–31], and we utilize the identical parameters and setup as in Ref. [31]. Modeling the FVTX acceptance and efficiency, we find reasonable agreement with the experimental FVTX track distribution and then calculate the $v_2\{2\}$ and $v_2\{4\}$ from AMPT as shown in Fig. 3. The AMPT calculations include event-by-event geometry fluctuations via Monte Carlo Glauber [32], flow (defined here as momentum anisotropy relative to the initial geometry), and nonflow. AMPT gives a reasonable

description of the magnitude and trend of $v_2\{4\}$, while underpredicting the $v_2\{2\}$; this may be due to an underestimation of the nonflow.

Our measurement of $v_2\{2\}$ is particularly susceptible to nonflow contributions because we allow combinations that may be close in pseudorapidity. Analyses of LHC data (e.g. Refs [15–18]) introduce a pseudorapidity gap $|\Delta\eta| > 2$ between all pairs thus reducing contributions from particle decays, intrajet correlations, etc. In our case, because of the FVTX acceptance, such an η gap

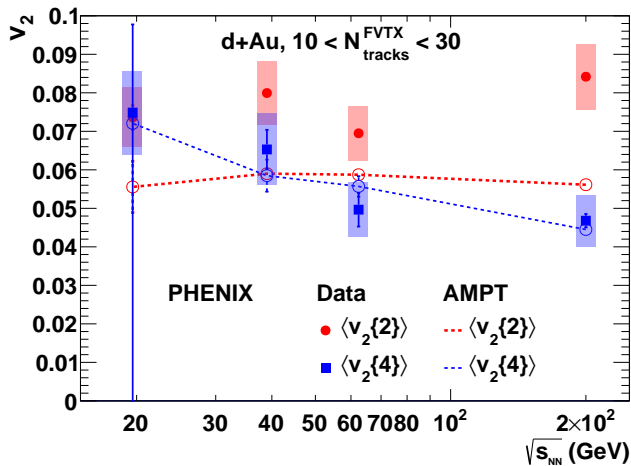


FIG. 3. $v_2\{2\}$ and $v_2\{4\}$ as a function of $\sqrt{s_{NN}}$ in $d+Au$ collisions. AMPT calculations are shown for comparison. For 19.6 GeV the confidence interval for $v_2\{4\}$ to be real is 79%.

necessitates requiring one particle per arm. In $d+Au$ collisions, particularly at the lower energies, this means that the kinematics for the $v_2\{2, |\Delta\eta| > 2\}$ and $v_2\{4\}$ are very different and the former will be strongly effected by asymmetries in v_2 between forward and backward rapidity, as well as longitudinal decorrelations [33, 34].

Nonetheless, we calculate $v_2\{2, |\Delta\eta| > 2\}$ and show the results in Fig. 2. We find that $v_2\{2, |\Delta\eta| > 2\} < v_2\{2\}$ for all four energies as expected from the reduction in nonflow contributions; however, we also find that $v_2\{2, |\Delta\eta| > 2\} < v_2\{4\}$, which cannot be reconciled within the context of Eqns. 10, 11 alone. In AMPT, the true v_2 at forward (d-going) rapidity v_2^F is significantly lower than v_2 at backward (Au-going) rapidity v_2^B . The $v_2\{2, |\Delta\eta| > 2\} = \sqrt{v_2^B v_2^F}$ whereas the $v_2\{4\}$ is heavily weighted towards v_2^B where there are more tracks in the FVTX. This difference in kinematic sensitivity makes a quantitative comparison with $v_2\{4\}$ challenging, while opening the door to new sensitivity to the longitudinal structure of the correlations.

Let us now return to the results in $p+Au$ collisions, where the $v_2\{4\}$ is complex. Following Eqn. 11, if the event-by-event v_2 fluctuations are larger in $p+Au$ compared with $d+Au$ to the extent that $\sigma > v_2$, this would explain the sign change. In the case of ideal hydrodynamic evolution, the flow v_2 is proportional to the initial elliptical geometric eccentricity ε_2 [35]. Thus, we show in Fig. 4 the ε_2 distributions from Monte Carlo Glauber calculations [32] for $p+Au$ and $d+Au$ at $\sqrt{s_{NN}} = 200$ GeV. The average ε_2 for $d+Au$ is almost twice the value for $p+Au$, and both distributions are highly nonGaussian. The ε_2 distribution in $p+Au$ collisions has large positive skew and the ε_2 distribution in $d+Au$ collisions is significantly platykurtic. The exact values of the skewness s and kurtosis k are listed in the figure. We can define cu-

mulants of ε_2 exactly as one does for the v_2 in Eqs. 4–9. If we do not restrict ourselves to the Gaussian approximation, but instead include all higher moments, we find $\varepsilon_2\{4\}$ values of 0.166 (0.508) in $p+Au$ ($d+Au$) collisions when using the exact form compared to 0.232 (0.505) in the Gaussian approximation. The conventional Gaussian approximation significantly overpredicts the exact calculation in $p+Au$, and slightly underpredicts it in $d+Au$. These geometry fluctuation contributions go in the right direction to reducing the magnitude of the $v_2\{4\}$ in $p+Au$ collisions, but not to the extent of flipping the sign of the cumulant and generating a complex $v_2\{4\}$.

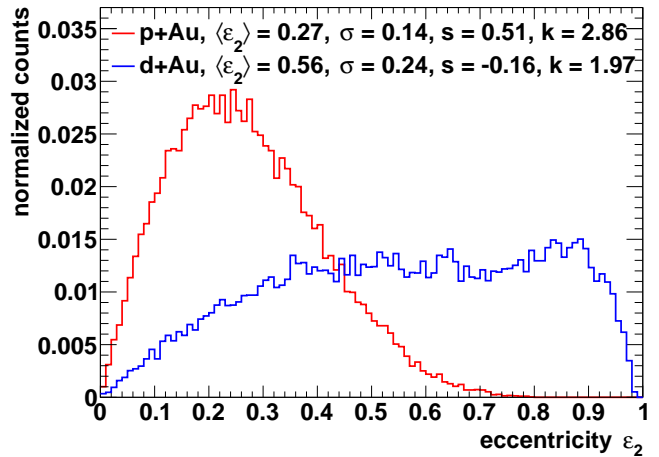


FIG. 4. Eccentricity distributions for $p+Au$ and $d+Au$ at $\sqrt{s_{NN}} = 200$ GeV as calculated via Monte Carlo Glauber. The exact values for the mean $\langle\varepsilon_2\rangle$, standard deviation σ , skewness s , and kurtosis k are listed on the figure in the caption for each distribution.

It is possible that fluctuations in translating the initial eccentricity into the final state momentum anisotropy lead to additional fluctuations in the v_2 values that could result in $c_2\{4\}$ becoming positive in $p+Au$ collisions. In fact, calculations utilizing AMPT, which describe the negative $c_2\{4\}$ and thus real $v_2\{4\}$ in $d+Au$, yield a positive valued $c_2\{4\}$ in $p+Au$ collisions, as shown by the green curves in Fig. 1. It is notable that these AMPT calculations utilize the identical Monte Carlo Glauber initial conditions as shown in Fig. 4, and thus this sign change is definitively from additional fluctuation effects.

In summary, we have presented measurements of v_2 from multiparticle correlations in $p+Au$ collisions at $\sqrt{s_{NN}} = 200$ GeV and in $d+Au$ collisions at $\sqrt{s_{NN}} = 200, 62.4, 39,$ and 19.6 GeV. We find real-valued $v_2\{4\}$ in $d+Au$ at all collision energies, providing evidence for collectivity in $d+Au$ at all energies. At the highest energy in $d+Au$, this evidence is further strengthened by the observation of $v_2\{4\} \approx v_2\{6\}$, indicating that nonflow contributions to $v_2\{4\}$ are subdominant. We find $v_2\{4\}$ is complex in $p+Au$ at $\sqrt{s_{NN}} = 200$ GeV. The ε_2 distribution in $p+Au$ is highly nonGaussian, leading to an $\varepsilon_2\{4\}$

much lower than Gaussian expectations. Additional fluctuations in the translation of ε_2 to v_2 may explain the observation of $v_2\{4\}$ being complex in p +Au. That collision systems with different initial geometries (p +Au and d +Au) at fixed collision energy (200 GeV) lead to significantly different cumulants indicates a geometrical and therefore collective origin of the correlations.

We thank the staff of the Collider-Accelerator and Physics Departments at Brookhaven National Laboratory and the staff of the other PHENIX participating institutions for their vital contributions. We acknowledge support from the Office of Nuclear Physics in the Office of Science of the Department of Energy, the National Science Foundation, Abilene Christian University Research Council, Research Foundation of SUNY, and Dean of the College of Arts and Sciences, Vanderbilt University (U.S.A), Ministry of Education, Culture, Sports, Science, and Technology and the Japan Society for the Promotion of Science (Japan), Conselho Nacional de Desenvolvimento Científico e Tecnológico and Fundação de Amparo à Pesquisa do Estado de São Paulo (Brazil), Natural Science Foundation of China (People's Republic of China), Croatian Science Foundation and Ministry of Science and Education (Croatia), Ministry of Education, Youth and Sports (Czech Republic), Centre National de la Recherche Scientifique, Commissariat à l'Énergie Atomique, and Institut National de Physique Nucléaire et de Physique des Particules (France), Bundesministerium für Bildung und Forschung, Deutscher Akademischer Austausch Dienst, and Alexander von Humboldt Stiftung (Germany), National Science Fund, OTKA, EFOP, and the Ch. Simonyi Fund (Hungary), Department of Atomic Energy and Department of Science and Technology (India), Israel Science Foundation (Israel), Basic Science Research Program through NRF of the Ministry of Education (Korea), Physics Department, Lahore University of Management Sciences (Pakistan), Ministry of Education and Science, Russian Academy of Sciences, Federal Agency of Atomic Energy (Russia), VR and Wallenberg Foundation (Sweden), the U.S. Civilian Research and Development Foundation for the Independent States of the Former Soviet Union, the Hungarian American Enterprise Scholarship Fund, and the US-Israel Binational Science Foundation.

* PHENIX Spokesperson: akiba@rcf.rhic.bnl.gov

† Deceased

- [1] K. Adcox *et al.* (PHENIX Collaboration), "Formation of dense partonic matter in relativistic nucleus nucleus collisions at RHIC: Experimental evaluation by the PHENIX collaboration," Nucl. Phys. A **757**, 184 (2005).
- [2] J. Adams *et al.* (STAR Collaboration), "Experimental and theoretical challenges in the search for the quark gluon plasma: The STAR collaboration's critical assessment of the evidence from RHIC collisions," Nucl. Phys. A **757**, 102 (2005).
- [3] B. B. Back *et al.* (PHOBOS Collaboration), "The PHOBOS perspective on discoveries at RHIC," Nucl. Phys. A **757**, 28 (2005).
- [4] I. Arsene *et al.* (BRAHMS Collaboration), "Quark gluon plasma and color glass condensate at RHIC? The perspective from the BRAHMS experiment," Nucl. Phys. A **757**, 1 (2005).
- [5] S. Chatrchyan *et al.* (CMS Collaboration), "Observation of long-range near-side angular correlations in proton-lead collisions at the LHC," Phys. Lett. B **718**, 795 (2013).
- [6] B. Abelev *et al.* (ALICE Collaboration), "Long-range angular correlations on the near and away side in p -Pb collisions at $\sqrt{s_{NN}} = 5.02$ TeV," Phys. Lett. B **719**, 29 (2013).
- [7] G. Aad *et al.* (ATLAS Collaboration), "Observation of Associated Near-Side and Away-Side Long-Range Correlations in $\sqrt{s_{NN}}=5.02$ TeV Proton-Lead Collisions with the ATLAS Detector," Phys. Rev. Lett. **110**, 182302 (2013).
- [8] A. Adare *et al.* (PHENIX Collaboration), "Quadrupole Anisotropy in Dihadron Azimuthal Correlations in Central d +Au Collisions at $\sqrt{s_{NN}}=200$ GeV," Phys. Rev. Lett. **111**, 212301 (2013).
- [9] A. Adare *et al.* (PHENIX Collaboration), "Measurement of long-range angular correlation and quadrupole anisotropy of pions and (anti)protons in central d +Au collisions at $\sqrt{s_{NN}}=200$ GeV," Phys. Rev. Lett. **114**, 192301 (2015).
- [10] A. Adare *et al.* (PHENIX Collaboration), "Measurements of elliptic and triangular flow in high-multiplicity ^3He +Au collisions at $\sqrt{s_{NN}} = 200$ GeV," Phys. Rev. Lett. **115**, 142301 (2015).
- [11] C. Aidala *et al.* (PHENIX Collaboration), "Measurement of long-range angular correlations and azimuthal anisotropies in high-multiplicity p +Au collisions at $\sqrt{s_{NN}} = 200$ GeV," Phys. Rev. C **95**, 034910 (2017).
- [12] V. Khachatryan *et al.* (CMS Collaboration), "Observation of Long-Range Near-Side Angular Correlations in Proton-Proton Collisions at the LHC," JHEP **09**, 091 (2010).
- [13] G. Aad *et al.* (ATLAS Collaboration), "Observation of Long-Range Elliptic Azimuthal Anisotropies in $\sqrt{s} = 13$ and 2.76 TeV pp Collisions with the ATLAS Detector," Phys. Rev. Lett. **116**, 172301 (2016).
- [14] V. Khachatryan *et al.* (CMS Collaboration), "Evidence for collectivity in pp collisions at the LHC," Phys. Lett. B **765**, 193 (2017).
- [15] G. Aad *et al.* (ATLAS Collaboration), "Measurement with the ATLAS detector of multi-particle azimuthal correlations in p +Pb collisions at $\sqrt{s_{NN}}=5.02$ TeV," Phys. Lett. B **725**, 60 (2013).
- [16] S. Chatrchyan *et al.* (CMS Collaboration), "Multiplicity and transverse momentum dependence of two- and four-particle correlations in p Pb and PbPb collisions," Phys. Lett. B **724**, 213 (2013).
- [17] B. B. Abelev *et al.* (ALICE Collaboration), "Multiparticle azimuthal correlations in p -Pb and Pb-Pb collisions at the CERN Large Hadron Collider," Phys. Rev. C **90**, 054901 (2014).
- [18] V. Khachatryan *et al.* (CMS Collaboration), "Evidence for Collective Multiparticle Correlations in p -Pb Colli-

- sions,” *Phys. Rev. Lett.* **115**, 012301 (2015).
- [19] C. Loizides, “Experimental overview on small collision systems at the LHC,” *Proceedings, 25th International Conference on Ultra-Relativistic Nucleus-Nucleus Collisions (Quark Matter 2015): Kobe, Japan, September 27-October 3, 2015*, *Nucl. Phys. A* **956**, 200 (2016).
- [20] K. Dusling, M. Mace, and R. Venugopalan, “Parton model description of multiparticle azimuthal correlations in pA collisions,” [ArXiv:1706.06260](https://arxiv.org/abs/1706.06260).
- [21] S. A. Voloshin and Y. Zhang, “Flow study in relativistic nuclear collisions by Fourier expansion of Azimuthal particle distributions,” *Z. Phys. C* **70**, 665 (1996).
- [22] A. Bilandzic, R. Snellings, and S. Voloshin, “Flow analysis with cumulants: Direct calculations,” *Phys. Rev. C* **83**, 044913 (2011).
- [23] J.-Y. Ollitrault, A. M. Poskanzer, and S. A. Voloshin, “Effect of flow fluctuations and nonflow on elliptic flow methods,” *Phys. Rev. C* **80**, 014904 (2009).
- [24] K. Adcox *et al.* (PHENIX Collaboration), “PHENIX detector overview,” *Nucl. Instrum. Methods Phys. Res., Sec. A* **499**, 469 (2003).
- [25] K. Ikematsu *et al.*, “A Start-timing detector for the collider experiment PHENIX at RHIC-BNL,” *Nucl. Instrum. Methods Phys. Res., Sec. A* **411**, 238 (1998).
- [26] C. Aidala *et al.*, “The PHENIX Forward Silicon Vertex Detector,” *Nucl. Instrum. Methods Phys. Res., Sec. A* **755**, 441 (2014).
- [27] A. M. Poskanzer and S. A. Voloshin, “Methods for analyzing anisotropic flow in relativistic nuclear collisions,” *Phys. Rev. C* **58**, 1671 (1998).
- [28] Z.-W. Lin, C. M. Ko, B.-A. Li, B. Zhang, and S. Pal, “A Multi-phase transport model for relativistic heavy ion collisions,” *Phys. Rev. C* **72**, 064901 (2005).
- [29] A. Bzdak and G.-L. Ma, “Elliptic and triangular flow in $p+Pb$ and peripheral $Pb+Pb$ collisions from parton scatterings,” *Phys. Rev. Lett.* **113**, 252301 (2014).
- [30] J. D. Orjuela Koop, A. Adare, D. McGlinchey, and J. L. Nagle, “Azimuthal anisotropy relative to the participant plane from a multiphase transport model in central $p+Au$, $d+Au$, and ^3He+Au collisions at $\sqrt{s_{NN}} = 200$ GeV,” *Phys. Rev. C* **92**, 054903 (2015).
- [31] J. D. Orjuela Koop, R. Belmont, P. Yin, and J. L. Nagle, “Exploring the Beam Energy Dependence of Flow-Like Signatures in Small System $d+Au$ Collisions,” *Phys. Rev. C* **93**, 044910 (2016).
- [32] C. Loizides, J. Nagle, and P. Steinberg, “Improved version of the PHOBOS Glauber Monte Carlo,” *SoftwareX* **1**, 13 (2015).
- [33] H. Petersen, V. Bhattacharya, S. A. Bass, and C. Greiner, “Longitudinal correlation of the triangular flow event plane in a hybrid approach with hadron and parton cascade initial conditions,” *Phys. Rev. C* **84**, 054908 (2011).
- [34] K. Xiao, F. Liu, and F. Wang, “Event-plane decorrelation over pseudorapidity and its effect on azimuthal anisotropy measurements in relativistic heavy-ion collisions,” *Phys. Rev. C* **87**, 011901 (2013).
- [35] J.-Y. Ollitrault, “Anisotropy as a signature of transverse collective flow,” *Phys. Rev. D* **46**, 229 (1992).